ACS Chemical Neuroscience

Research Article

pubs.acs.org/chemneuro

Selectivity Optimization of Substituted 1,2,3-Triazoles as α7 Nicotinic Acetylcholine Receptor Agonists

Kuntarat Arunrungvichian,[†,‡,§] Valery V. Fokin,[§] Opa Vajragupta,*[,†] and Palmer Taylor[‡]

[†]Center of Excellence for Innovation in Drug Design and Discovery, Faculty of Pharmacy, Mahidol University, 447 Sri-Ayudhya Road, Bangkok 10400, Thailand

[‡]Department of Pharmacology, Skaggs School of Pharmacy and Pharmaceutical Sciences, University of California, San Diego, 9500 Gilman Drive, La Jolla, California 92093-0650, United States

[§]Department of Chemistry, The Scripps Research Institute, 10550 North Torrey Pines Road, La Jolla, California 92037, United States

Supporting Information

ABSTRACT: Three series of substituted *anti*-1,2,3-triazoles (IND, PPRD, and QND), synthesized by cycloaddition from azide and alkyne building blocks, were designed to enhance selectivity and potency profiles of a lead α7 nicotinic acetylcholine receptor (α7-nAChR) agonist, TTIn-1. Designed compounds were synthesized and screened for affinity by a radioligand binding assay. Their functional characterization as agonists and antagonists was performed by fluorescence resonance energy transfer assay using cell lines expressing transfected cDNAs, α7-nAChRs, α4β2-nAChRs, and $5HT_{3A}$ receptors, and a fluorescence cell reporter. In the IND series, a tropane ring of TTIn-1, substituted at N1, was replaced by mono- and bicyclic amines to vary length and conformational flexibility of a carbon linker between nitrogen atom and N1 of the triazole. Compounds with a two-carbon atom linker optimized binding with K_d's at the submicromolar level. Further modification at the hydrophobic indole of TTIn-1 was made in PPRD and QND series by fixing the amine center with the highest affinity building blocks in the IND series. Compounds from IND and PPRD series are selective as agonists for the α7-nAChRs over α4β2-nAChRs and $5HT_{3A}$ receptors. Lead compounds in the three series have EC_{50}'s between 28 and 260 nM. Based on the EC_{50}, affinity, and selectivity determined from the binding and cellular responses, two of the leads have been advanced to behavioral studies described in the companion article (DOI: 10.1021/acschemneuro.5b00059).

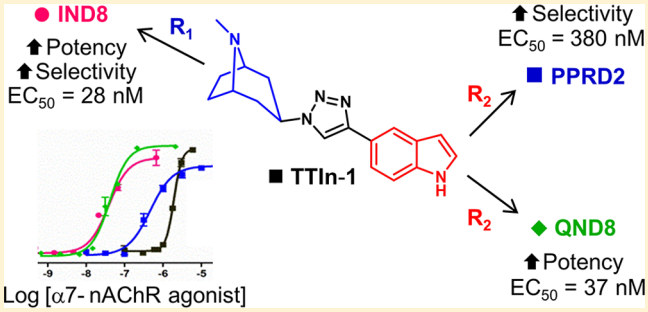

KEYWORDS: *Neurologic disorders, α7-nAChRs, cycloaddition reactions, triazole, click-chemistry, nicotinic acetylcholine receptors, pentameric ligand-gated ion channels*

Nicotinic acetylcholine receptors (nAChRs) are widely distributed in the central and peripheral nervous systems (CNS and PNS), controlling peripheral voluntary motor, autonomic, and central nervous system functions.[1] Since they are found in abundance in presynaptic locations in the CNS, they can control release of other transmitters as well as acetylcholine itself. Therefore, they have diverse modulatory functions and are candidate targets for neurologic disorders of development, schizophrenia and autism, and the aging process, Parkinsonism and the Alzheimer dementias.[2−4]

Structurally, nAChRs are members of the pentameric Cys-loop ligand-gated ion channel (LGIC) superfamily, which are composed of five transmembrane spanning subunits, assembled to surround a centrosymmetric ion pore. There are at least 12 distinct neuronal subunits (α2−α10 and β2−β4) characterized in mammalian and avian systems.[1,5] Structures of these pentameric receptors are divided into three domains: N-terminal extracellular, transmembrane, and intracellular. Assembly of nAChRs is specific for certain subunit partnerships, and can be categorized as hetero- and homopentameric. Differences in subunit combinations and localization lead to their functional and pharmacological variances.[6,7] The orthosteric ligand binding pocket is located at the interface in the extracellular domain between a principal (alpha) and a complementary subunit.[8] The α7-nAChR is unique in being homomeric with identical binding sites formed between its principal, C loop containing face and the opposing face of the neighboring subunit.

Several α7-nAChR agonists have been developed for clinical trials, namely, GTS-21,[9,10] MEM3454,[11] TC-5619,[12] PNU-282987,[13] AR-R17779,[14] ABT-107,[15] and SEN34625/WYE-103914[16] (Figure 1). For α7-nAChR agonist design, the primary pharmacophoric features of α7-nAChR agonists, a cationic center, a hydrogen-bond acceptor, and a hydrophobic moiety were modified.[14,17,18] Despite comprehensive structural

Received: February 11, 2015
Published: May 1, 2015

DOI: 10.1021/acschemneuro.5b00058
ACS Chem. Neurosci. 2015, 6, 1317−1330

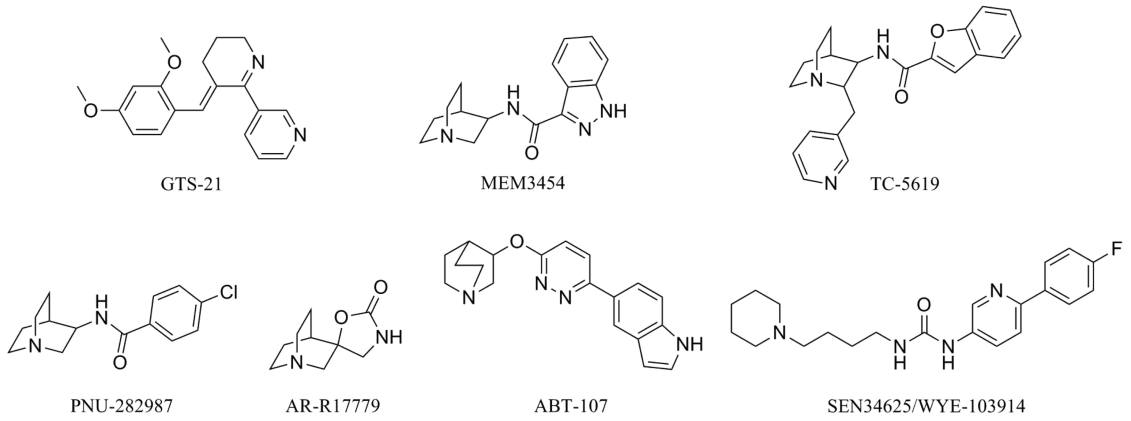

Figure 1. α7-nAChR agonist prototypes.

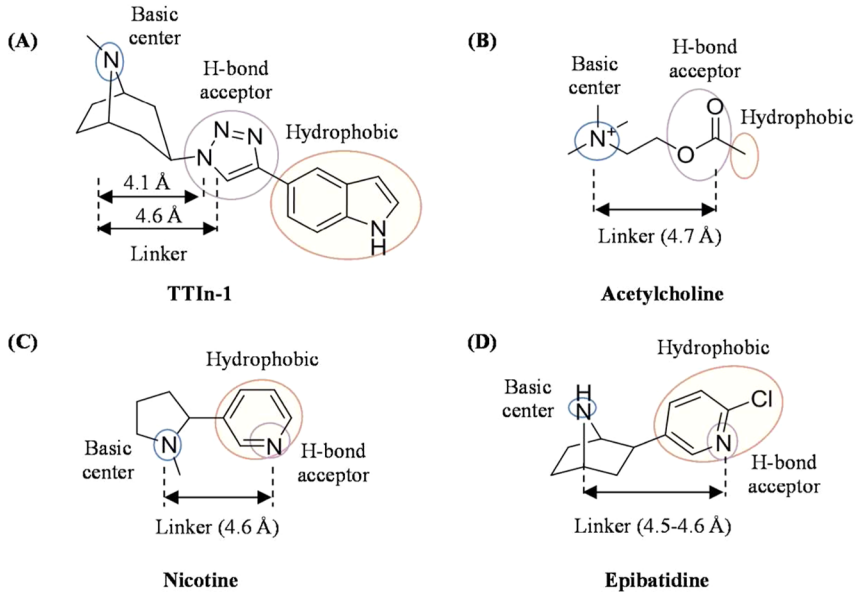

Figure 2. α7-nAChR agonist pharmacophore. (A) lead compound TTIn-1, (B) acetylcholine (PDB ID: 3WIP), (C) nicotine (PDB ID: 1UW6), and (D) epibatidine (PDB ID: 2BYQ, 3SQ6) with pharmacophore map.

studies, limitations in the development of α7-nAChR agonists, encompassing selectivity, stability, and toxicity, remain.[12,19]

The availability of a soluble extracellular domain surrogate of the homomeric α7-nAChR enables one to synthesize candidate triazole ligands from azide and alkyne building blocks on a homologous relative of the receptor target of drug action, the acetylcholine binding protein (AChBP). These lead products can be identified and determined structures of the complexes with AChBP by mass spectrometry.[20] Structural permutations of these leads can be synthesized in small quantities and in the absence of template by metal-catalyzed cycloadditions.[21] The copper-catalyzed azide−alkyne cycloaddition (CuAAC) has several advantages: regiospecificity, requirements for only stoichiometric amounts of starting materials for reaction completion, reaction conditions paralleling biological temperatures, and ease of reaction and product purification.[22,23]

anti-1,2,3-Triazole-containing molecules from metal catalyzed click chemistry have been reported to stimulate α7-nAChRs as agonists[24,25] and antagonize $\alpha4\beta2$-nAChRs and $5HT_{3A}$ receptors.[21] The N2 and N3 of the triazole ring serve as uncharged H-bond acceptors, and the triazole ring itself serves as a stable, uncharged linker between the cationic center and the hydrophobic ring.[20,22]

In this study, the cationic center and aromatic indole of the triazole-based lead compound, TTIn-1 (Figure 2A), were modified to improve the selectivity and potency profiles to α7-nAChRs. Tertiary amines that can cross the blood-brain barrier (BBB) and be protonated in the CNS were chosen to mimic the cationic center in the α7-nAChR pharmacophore. Critical interactions to stabilize the nicotinic ligand are either a cation−π interaction for quaternary amine with an enveloping cage of aromatic side chains or a H-bond interaction from a protonated secondary or tertiary amine or an imine to carbonyl backbone oxygen of a conserved tryptophan.[26] The carbon chain between the cationic center and the H-bond acceptor or the triazole was varied to optimize connecting length to maintain both H-bond interactions from the chosen basic tertiary amine and the triazole with amino acid residues forming the binding pocket of α7-nAChRs. The role of functional group in the hydrophobic region, where the uncharged pyridine of nicotine or epibatidine resides,[27,28] was studied as well. Receptor binding and functional assays of synthesized compounds were carried out by radioligand binding and

DOI: 10.1021/acschemneuro.5b00058
ACS Chem. Neurosci. 2015, 6, 1317−1330

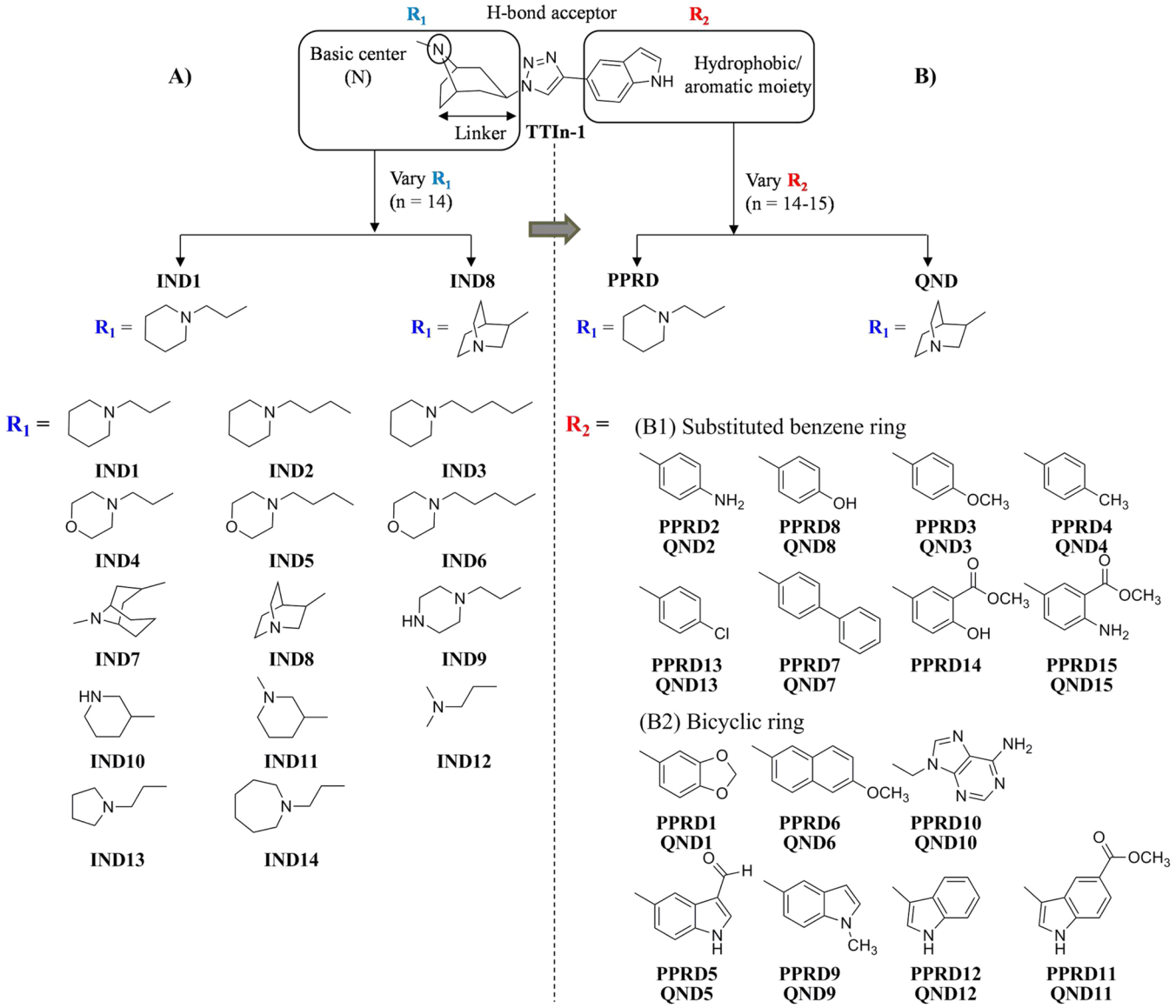

Figure 3. Optimization of the lead compound, TTIn-1.

fluorescence resonance energy transfer (FRET) assays, respectively, on intact cells in culture expressing α7-nAChRs, $\alpha4\beta2$-nAChRs, and $5HT_{3A}$ receptors.

RESULTS AND DISCUSSION

1. Design Strategies. The lead tertiary amine TTIn-1 was optimized based on projected components of an α7-nAChR pharmacophore (Figure 2) which encompasses (i) the basic center with its linker (R_1 of IND series) and (ii) hydrophobic aromatic moieties (R_2 of PPRD and QND series) as shown in Figure 3.

In the first set of 14 compounds (Figure 3A), the basic center was the prime focus. The tropane of TTIn-1 was replaced with different amine fragments: (i) simple alicyclic rings (IND1–IND6, IND9), that is, piperidine, morpholine, and piperazine; (ii) fused alicyclic ring (IND7, IND8); (iii) semirigid analogues of two-carbon linker (IND10, IND11); (iv) fully flexible aliphatic amine (IND12); and (v) reduced and enlarged alicyclic rings (IND13, IND14). Modifications were made to investigate distances spanning the basic nitrogen and the triazole ring, the flexibility or spatial configuration, and the steric hindrance on the binding affinity and potency. Projected distances between the basic nitrogen atom and the triazole N1 of the designed compounds were in the range of two to four C–C bonds (3.7–6.4 Å) based on structures of acetylcholine (2 C atoms, 4.7 Å, Figure 2B) and SEN34625/WYE-103914[16] (4 C atoms, 7.9 Å between the piperidine N and urea NH, Figure 1). Simple monocyclic amines (IND1–IND6) with lower pK_a values of 6.93–9.66 (Table 1) were chosen to replace the tropane ring of TTIn-1 (pK_a 9.67) for pharmacokinetic advantages. Once the unprotonated amine crosses the blood-brain barrier, the pharmacologically active protonated state forms that is required for hydrogen bond donation to the backbone carbonyl of a conserved Trp on the principal face of the nAChR.[26] Therefore, the pK_a should accommodate a balance of blood-brain penetration (pharmacokinetics) and receptor binding of the protonated species (pharmacodynamics). Other alicyclic rings, bicyclic analogs and ring size reduction and expansion were employed. The number of carbon atoms between the basic amine N and the triazole ring was fixed at two or three C atoms.

DOI: 10.1021/acschemneuro.5b00058
ACS Chem. Neurosci. 2015, 6, 1317–1330

Table 1. Physicochemical Properties and Distance between Basic Amine and N1 and N2 of Triazole Ring[a]

					3.8 Å			3.7 Å		
compd	pK_a	log P	distance to N1 (Å)	distance to N2 (Å)	compd	pK_a	log P	compd	pK_a	log P
TTIn-1	9.67	2.7	4.1	4.6	PPRD1	9.13	2.55	QND1	9.17	2.05
IND1	9.13	3.02	**3.8**	**4.8**	PPRD2	9.14, 3.18	2.09	QND2	9.17, 3.12	1.6
IND2	9.66	3.08	5.1	6.1	PPRD3	9.13	2.76	QND3	9.17	2.27
IND3	9.65	3.6	6.4	7.3	PPRD4	9.13	3.44	QND4	9.17	2.94
IND4	6.93	1.95	3.8	4.5	PPRD5	9.13	2.73	QND5	9.17	2.24
IND5	7.46	2.01	5.1	6.1	PPRD6	9.13	3.75	QND6	9.17	3.26
IND6	7.45	2.53	6.4	7.3	PPRD7	9.13	4.57	QND7	9.17	4.08
IND7	9.54	3.15	3.8	4.8	PPRD8	8.9	2.62	QND8	8.93	2.13
IND8	9.17	2.53	**3.7**	**4.1**	PPRD9	9.13	3.24	QND9	9.17	2.75
IND9	9.28, 4.65	1.63	3.8	4.8	PPRD10	8.70, 5.11	0.41	QND10	9.09, 5.11	−0.08
IND10	9.67	2.25	3.8	4.5	PPRD11	9.11	3.02	QND11	9.17	2.53
IND11	8.85	2.64	3.8	4.5	PPRD12	9.12	3.02	QND12	9.17	2.53
IND12	8.63	2.17	3.8	4.7	PPRD13	9.13	3.53	QND13	9.17	3.03
IND13	9.26	2.58	3.8	4.8	PPRD14	9.4	3.27			
IND14	9.59	3.47	3.8	4.5	PPRD15	9.14, 1.07	2.75	QND15	9.17, 1.06	2.25

[a]Distance between basic amine and N1 of triazole ring of 3D structures cleaned by MarvinSketch was measured with PyMOL. The physicochemical properties were predicted by MarvinSketch.

Scheme 1. Synthesis of the Azide Building Blocks[a]

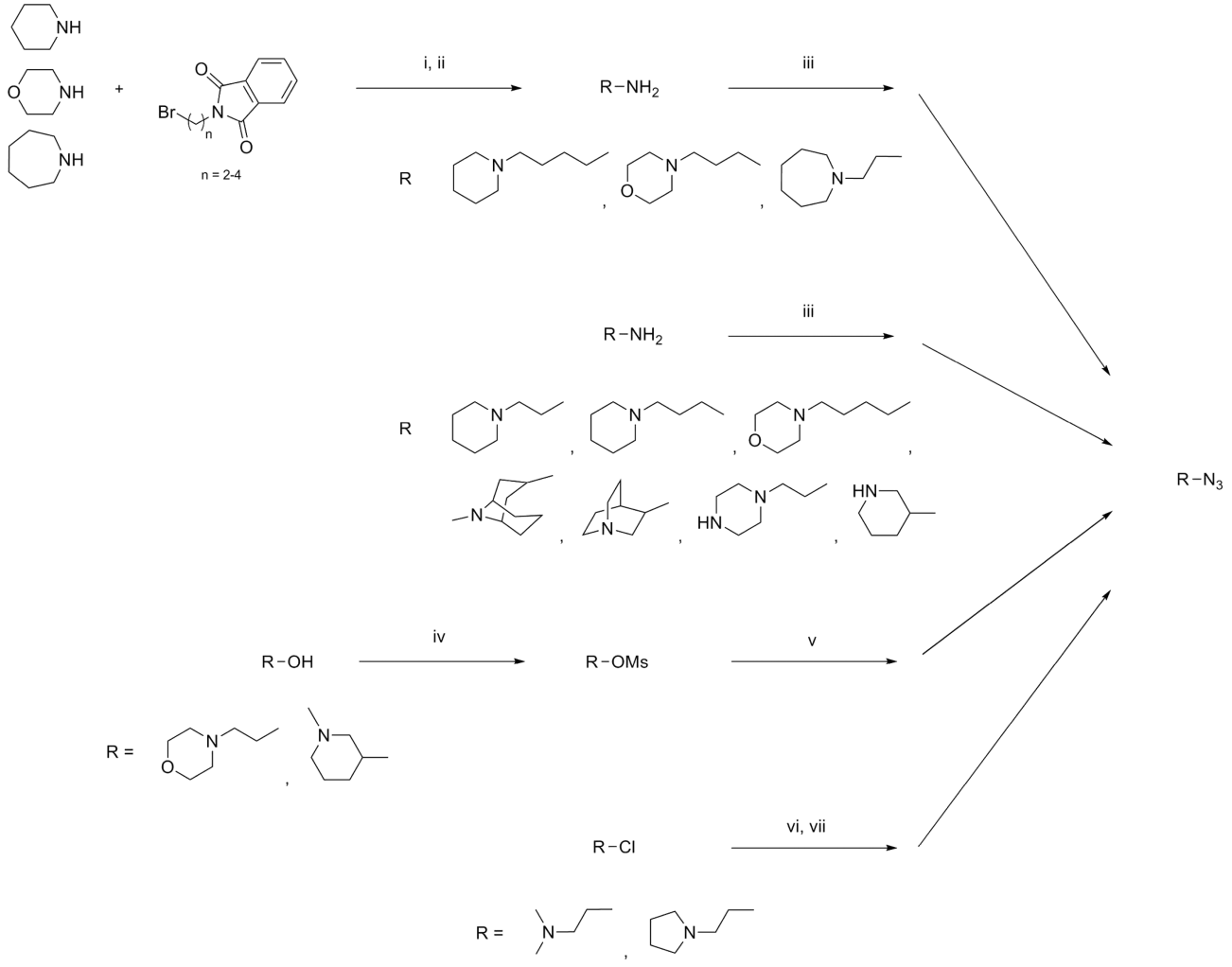

[a]Reagents and conditions: (i) Et_3N, EtOH, reflux, overnight; (ii) $H_2N{-}NH_2$, EtOH, reflux 45 min; (iii) freshly prepared TfN_3 in toluene, K_2CO_3, $CuSO_4{\cdot}5H_2O$, H_2O:CH_3OH, RT, overnight; (iv) CH_3SO_2Cl, Et_3N, CH_2Cl_2, 0 °C to RT, 4 h; (v) NaN_3, MeCN, reflux, 6 h; (vi) NaN_3, H_2O, reflux, overnight; (vii) NaOH, Et_2O, 0 °C, 30 min.

DOI: 10.1021/acschemneuro.5b00058
ACS Chem. Neurosci. 2015, 6, 1317−1330

Scheme 2. Synthesis of Terminal Alkynes[a]

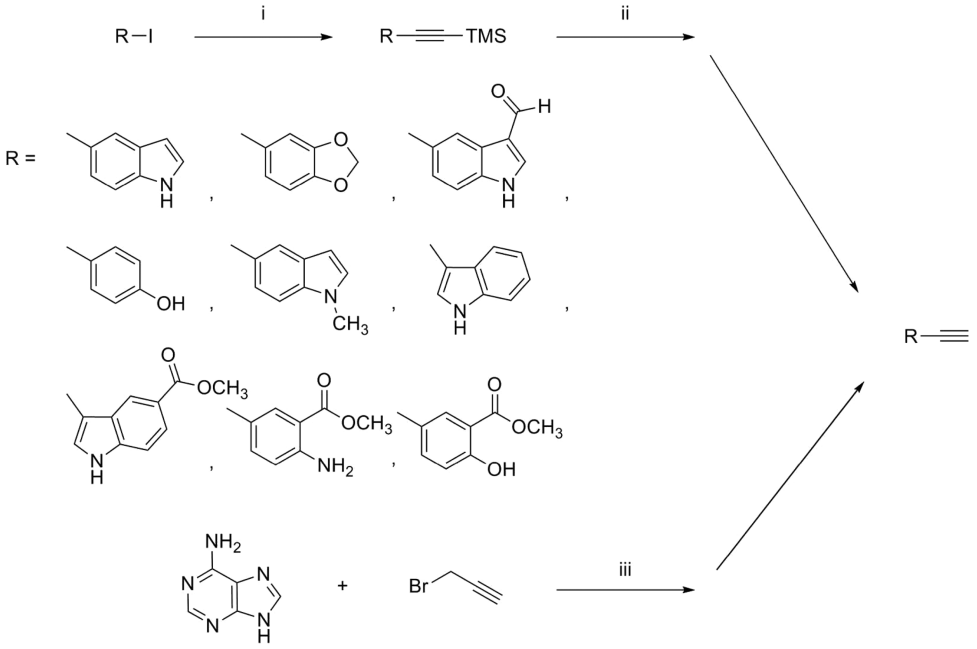

[a]Reagents and conditions: (i) TMS—C≡CH, CuI, $PdCl_2(PPh_3)_2$, DMF, RT, overnight; (ii) TBAF in THF or K_2CO_3 in CH_3OH, RT, 1 h; (iii) K_2CO_3, DMF, RT, overnight.

Scheme 3. Synthesis of *anti*-1,2,3-Triazole Containing Molecules

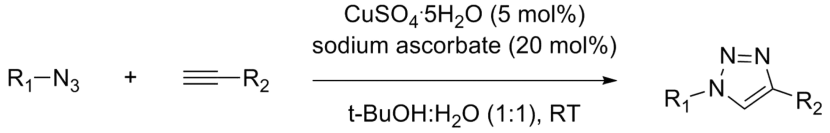

In the second set of 29 compounds in the R_2 series (Figure 3B), R_1 residues were fixed with leads from the first compound set that showed higher binding affinity to α7-nAChR (K_d < 0.34 μM), R_1 of the PPRD series is the 2-(piperidin-1-yl)ethyl moiety of IND1 and that for the QND series is the quinuclidine of IND8. The aromatic R_2 of both series was separated into two general categories, (i) mono- and disubstituted benzenes and (ii) bicyclic aromatic systems: indole and substituted indole, naphthalene and adenine rings. For the first category (Figure 3-B1), the *p*-position of the benzene ring was substituted with H-bond donors (−NH_2 and −OH), H-bond acceptor (−OCH_3), or groups of different electronic influence on the ring system (−CH_3, −Cl, −Ph) to verify the role of functional group at *p*-position of benzene ring. The *m*-substitution of a carboxy methyl ester was included in the structures of PPRD14, PPRD15, and QND15 to study the effect from the additional heteroatom substitution. For the second category (Figure 3-B2), the indole ring was modified by ring substitutions and linkage to the triazole.

Predicted physicochemical properties (pK_a, log *P*) and distance between basic nitrogen atom and N1 of triazole ring of compounds in IND, PPRD, and QND series are shown in Table 1.

2. Synthesis. The general synthesis of the designed compounds started with the synthesis of azide and alkyne building blocks followed by the CuAAC reaction,[20] yielding the final compounds as shown in Schemes 1−3. Azide building blocks were prepared by two different methods: the diazo transfer reaction of amine[29] for azide building blocks of IND1−IND3, IND5−IND10, IND14, PPRD1−PPRD15, QND1−QND13 and QND15, and the nucleophilic substitution of a leaving group with sodium azide[30,31] for azide building blocks of IND4, IND11−IND13. Then, the azide building blocks were reacted with the terminal alkynes that are commercially available or were prepared in house by the Sonogashira cross-coupling reaction[32] or nucleophilic substitution to yield 1,2,3-triazoles with 20−95% yield.

3. Biological Evaluation. The binding affinities ($1/K_d$) of all synthesized compounds were evaluated in cell based neurotransmitter fluorescent engineered reporter (CNiFERs) expressing α7-nAChRs, $\alpha4\beta2$-nAChRs, and $5HT_{3A}$ receptors. Ligand binding was assayed by competitive radioligand displacement using [^{3}H]-(±)-epibatidine for α7- and $\alpha4\beta2$-nAChRs and [^{3}H]-granisetron for $5HT_{3A}$ receptors. The $\alpha7/5HT_{3A}$ chimeric receptor, having an α7-nAChR extracellular domain and $5HT_{3A}$ transmembrane and cytoplasmic domains, was used instead of α7-nAChRs because the signal-to-noise ratio of the $\alpha7/5HT_{3A}$ chimeric receptors was significantly higher than the α7-nAChRs. Also, the chimeric receptors produced more robust and reproducible results (data not shown). Compounds at 10 μM concentration that competitively dissociated [^{3}H]-(±)-epibatidine or [^{3}H]-granisetron binding to LGIC-CNiFERs more than 50% were further analyzed over a range of concentrations for K_d values. Otherwise their K_d values are listed as >10 μM.

Compounds were functionally screened as agonists and antagonists, for selectivity and potency using FRET assay of LGIC-CNiFERs transfected cells.[33] All LGIC-CNiFERs for

DOI: 10.1021/acschemneuro.5b00058
ACS Chem. Neurosci. 2015, 6, 1317−1330

Table 2. Dissociation Constants for Ligand Binding, K_d, Activation Parameters, EC_{50}, and Functional Antagonism, K_A, Values of Indole Series (IND1−IND14), the Lead Compound TTIn-1, and the Reference α7-nAChR Agonist PNU-282987 from the Intact Cell Binding Assay (K_d) and FRET Assay Using LGIC-CNiFERs[a]

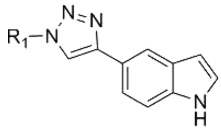

Compound	R_1	Binding affinity			Functional properties			
		$K_d \pm SD$ (μM)			Agonist $EC_{50} \pm SD$ (μM)		Antagonist $K_A \pm SD$ (μM)	
		α7	α4β2	$5HT_{3A}$	α7	$5HT_{3A}$	α4β2	$5HT_{3A}$
PNU-282987	-	0.27 ± 0.14	>10	>10	0.11 ± 0.01	-	>10	1.19 ± 0.34^{C}
TTIn-1[35]		$4.3 \pm 2.9^{\S}$	>10	6.0 ± 0.8	$0.57 \pm 0.13^{\S}$	-	2.7 ± 0.4^{C}, 11.5 ± 1.7^{NC}	6.1 ± 0.7^{NC}, 4.9 ± 2.7^{NC}
IND1		$0.34 \pm 0.13^{\#,\delta}$	>10	5.5 ± 1.4	$0.17 \pm 0.05^{\delta}$	>10	>10	>10
IND2		7.2 ± 1.3	>10	8.2 ± 3.4	2.2 ± 0.7	>10	>10	>10
IND3	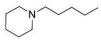	$13.8 \pm 4.1^{\#}$	>10	>10	0.91 ± 0.20	>10	>10	>10
IND4		>10	>10	>10	>10	>10	>10	>10
IND5		>10	>10	>10	>10	>10	>10	>10
IND6	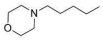	$14.1 \pm 0.3^{\#}$	>10	>10	$12.2 \pm 3.5^{\#}$	>10	>10	>10
IND7		4.5 ± 1.2	>10	$21.7 \pm 11.8^{\#}$	1.0 ± 0.3	>10	22.2 ± 6.9^{NC}	>10
IND8		$0.12 \pm 0.06^{\#,\delta}$	0.75 ± 0.20	$0.052 \pm 0.008^{\delta}$	$0.028 \pm 0.010^{\delta}$	0.21 ± 0.08*	>10	-
IND9		>10	>10	>10	$12.0 \pm 1.9^{\#}$	-	>10	4.7 ± 2.0^{C}, 3.0 ± 0.7^{NC}
IND10		3.0 ± 0.2	>10	3.4 ± 0.6	0.66 ± 0.16	-	>10	$1.0 \pm 0.3^{C,\#}$, 9.3 ± 5.0^{NC}
IND11		5.1 ± 1.4	>10	5.7 ± 1.5	3.3 ± 0.7	>10	>10	>10
IND12		7.7 ± 3.0	>10	2.9 ± 0.5	$5.7 \pm 1.1^{\#}$	-	>10	$3.2 \pm 0.4^{C,\#}$, 4.9 ± 1.5^{NC}
IND13		4.8 ± 0.9	>10	>10	2.2 ± 0.4	>10	>10	>10
IND14		1.1 ± 0.3	>10	9.3 ± 2.4	0.78 ± 0.16	-	>10	$2.7 \pm 1.1^{C,\#}$

[a]Data were analyzed from at least three independent experiments with each experiment containing two or more samples. Values are reported as means ± standard deviation (SD). K_d > 10 μM, EC_{50} > 10 μM, and K_A > 10 μM were indicated for the compounds that did not pass the initial screening for binding affinity and functional characterization. *partial agonist; ^{C}competitive antagonist; ^{NC}noncompetitive antagonist; $^{\#}p < 0.05$ compared with TTIn-1; $^{\S}p < 0.05$ compared with PNU-282987 from subanalysis; $^{\delta}p < 0.05$ compared with TTIn-1 from subanalysis. Values are calculated as described in Methods.

functional characterization are the same as those used for the competitive radioligand binding with the exception that α7-nAChRs were used instead of the aforementioned chimeric receptor. Initially, the agonist properties of tested compounds (final concentration = 13.3 μM) were assessed directly. Then, antagonism was subsequently evaluated (final concentration = 10 μM) by adding the standard agonists, (±)-epibatidine for α7- and α4β2-nAChRs and 5-hydroxytryptamine (5-HT) for $5HT_{3A}$ receptors. All α7-nAChR functional assays were performed in the presence of PNU-120596, an α7-nAChR positive allosteric modulator (PAM), to increase signal and delay formation of the desensitized state of α7-nAChRs. This

DOI: 10.1021/acschemneuro.5b00058
ACS Chem. Neurosci. 2015, 6, 1317−1330

addition enables measurement of more prolonged FRET signals.[33] Compounds having agonist responses of ≥0.20 of the maximal response were determined for EC_{50}, and compounds having inhibition fraction of ≥0.50 were determined for K_A.[21] Compounds with EC_{50} and K_A values >10 μM were not taken for further quantitation of receptor occupation and responses.

4. Effect of Variation in Basic Amine Ring System (IND Series). *4.1. Effect on Binding Affinity ($1/K_d$) or Dissociation Constant (K_d).* K_d values with α7-nAChRs as shown in Table 2 indicate that two compounds (IND1, IND8) exhibited statistically enhanced affinity or lower K_d for the α7-nAChRs (K_d = 0.34 and 0.12 μM, respectively) relative to the lead compound, TTIn-1[35] (K_d = 4.3 μM). When compared the binding affinity between these three compounds (TTIn-1, IND1, IND8) and PNU-282987, a reference α7-nAChR agonist, the K_d values reveal that the affinity of TTIn-1 is lower ($p < 0.05$), but the of IND1 and IND8 are not significantly different from PNU-282987 (K_d = 0.27 μM).

A comparison of K_d values indicated that extending the distance between the basic nitrogen and the triazole ring increased the K_d for α7-nAChRs: IND2 (length 5.1 Å, K_d = 7.2 μM) and IND3 (length 6.4 Å, K_d = 13.8 μM) compared with IND1 (3.8 Å linker length, K_d = 0.34 μM). Besides linker elongation, the additional heteroatom (IND4−IND6, IND9) in the simple alicyclic ring dramatically increases K_d for α7-nAChRs. This is probably due to (i) the lower pK_a of IND4−IND6 leading to a smaller fraction of the protonated forms (25−54%) forming H-bond to the backbone carbonyl of the conserved tryptophan on the principal face of the alpha subunit, or (ii) protonation of the secondary amine of IND9 at pH 7.4 resulting in an excessive distance (6.6 Å). Both of the fused alicyclic rings in this study (IND7, IND8) interact with α7-nAChRs, but only IND8 has the lower dissociation constant. The lower K_d of IND8 might come from the optimal distance to maintain both hydrogen bond interactions of IND8. Other modifications, that is, semirigid analogue (IND10, IND11), freely flexible aliphatic amine (IND12), and ring size alteration (IND13, IND14) did not appreciably affect the K_d for α7-nAChRs.

Most compounds that are able to interact with α7-nAChRs also bind to $5HT_{3A}$ receptors as may be expected from the sequence homology (Supporting Information Figure S1),[11,34] but there is a far smaller crossover to the α4β2-nAChRs where only IND8 showed a low K_d.

4.2. Effect of Basic Amine Center on Agonist and Antagonist (Pharmacologic Activity). The α7-nAChR agonist potencies are in general agreement with the binding affinities. EC_{50} values of agonists and K_A values of antagonists are shown in Table 2. α7-nAChR dose−response curves of IND1−IND14 are shown in Figure 4.

Only IND1 and IND8 are more potent than TTIn-1, with EC_{50} values of 0.17 and 0.028 μM versus 0.57 μM, respectively, and comparable to PNU-282987 (EC_{50} 0.11 μM). The higher potency profile of IND1 and IND8 over other alicyclic amines may arise from the stronger base of piperidine (pK_a 9.13) as well as quinuclidine (pK_a 9.17) and optimizing distance between basic amine and N1 of triazole (3.7−3.8 Å) to facilitate H-bond formation in the binding pocket of α7-nAChRs. However, compounds IND10−IND14, which have the same 3.8 Å distance, did not show enhanced α7-nAChR potency. This indicates that other factors such as flexibility and steric constraints govern the potency of α7-nAChR agonist.

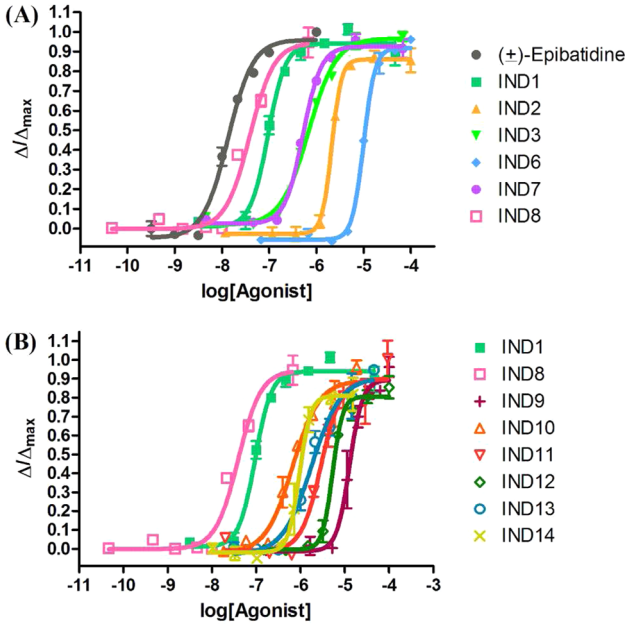

Figure 4. α7-nAChR agonist dose−response curves of (A) IND1−IND3, IND6−IND8 and (B) IND9−IND14. The α7-nAChR functional assays were conducted in the presence of 10 μM PNU-120596. FRET ratios were normalized to the maximum response by 100 nM (±)-epibatidine. The concentration−response curves show Hill coefficients of ∼2, but because of the limited concentration points and rapid responses, we have not estimated Hill coefficients for the 13 agonists.

For α4β2-nAChRs, IND7 showed noncompetitive antagonism with low potency profile ($K_A = 22.2^{NC}$ μM) (Supporting Information Figure S2). Surprisingly, IND8 showed high affinity binding to α4β2-nAChRs, but did not elicit agonist or antagonist properties. It is possible that the interacting residues are not the key residues of α4β2-nAChRs responsible for gating the cation channel.

The $5HT_{3A}$ functional responses for 8 of 14 compounds did not correlate well with the binding affinity measurements. Some compounds, that is, IND1, IND2, and IND7 apparently bound to $5HT_{3A}$ receptors, but did not yield detectable agonist or antagonist responses. Interestingly, one compound (IND8) turned out to be $5HT_{3A}$ partial agonist (EC_{50} = 0.21 μM). $5HT_{3A}$ receptor agonist and antagonist dose−response curves are shown in Supporting Information Figures S3 and S4.

The significant improvement of selectivity and potency profiles of IND1 and IND8 over the lead compound indicates that 3.7−3.8 Å is an optimal distance between the basic nitrogen atom and N1 of the triazole ring for α7-nAChR agonist activity. IND1, a six-membered monocyclic ring with a 2 methylene linker, is the most potent α7-nAChR agonist (EC_{50} = 0.17 μM) and highly selective for α7 over the α4β2-nAChR, and the $5HT_{3A}$ receptor. IND8, a bicyclic amine, is the most potent compound in the series (EC_{50} = 0.028 μM), but with a diminished degree of receptor selectivity. Therefore, the piperidine and quinuclidine rings from IND1 and IND8 representing mono- and bicyclic rings were selected as the cation center (R_1) for further modification of the hydrophobic R_2 in the second compound set, PPRD and QND series, respectively.

5. Variation in Aromatic Indole Substitution of the *anti*-Triazole (PPRD and QND Series). *5.1. Effect on*

DOI: 10.1021/acschemneuro.5b00058
ACS Chem. Neurosci. 2015, 6, 1317−1330

Table 3. K_d Values of Compounds in PPRD and QND Series from Intact Cell Binding Assay Using LGIC-CNiFERs[a]

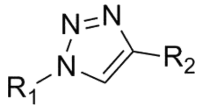

R_2	R_1 =	$K_d \pm$ SD (uM)			R_1 =	$K_d \pm$ SD (uM)		
		α7	α4β2	$5HT_{3A}$		α7	α4β2	$5HT_{3A}$
	IND1	0.34 ± 0.13	>10	5.5 ± 1.4	**IND8**	0.12 ± 0.06	0.75 ± 0.20	0.052 ± 0.008
Mono- and di-substituted benzenes								
NH_2	**PPRD2**	1.3 ± 0.4	>10	>10	**QND2**	0.32 ± 0.09	>10	1.2 ± 0.2[§]
OCH_3	**PPRD3**	15.5 ± 3.6[#]	>10	>10	**QND3**	0.20 ± 0.05	>10	2.3 ± 0.3[§]
CH_3	**PPRD4**	3.6 ± 1.3	>10	>10	**QND4**	0.36 ± 0.14	>10	0.14 ± 0.01
	PPRD7	>10	>10	>10	**QND7**	>10	>10	>10
OH	**PPRD8**	7.4 ± 1.6	>10	>10	**QND8**	0.081 ± 0.029	>10	0.54 ± 0.05[§]
Cl	**PPRD13**	31.9 ± 10.0[#]	>10	>10	**QND13**	0.36 ± 0.11	>10	0.40 ± 0.06
OCH_3, OH	**PPRD14**	>10	>10	1.9 ± 0.6[#]				
OCH_3, NH_2	**PPRD15**	4.4 ± 0.9	>10	>10	**QND15**	3.6 ± 1.3[§]	>10	0.043 ± 0.002
Bicyclic ring systems								
	PPRD1	11.3 ± 0.6[#]	>10	>10	**QND1**	0.16 ± 0.07	>10	0.048 ± 0.009
	PPRD5	3.3 ± 1.4[#]	>10	>10	**QND5**	2.8 ± 0.7[§]	>10	0.12 ± 0.04
OCH_3	**PPRD6**	>10	>10	>10	**QND6**	5.6 ± 0.5[§]	1.4 ± 0.2	>10
CH_3	**PPRD9**	12.1 ± 1.1[#]	>10	>10	**QND9**	1.9 ± 0.0[§]	1.3 ± 0.4	0.15 ± 0.03
NH_2	**PPRD10**	>10	>10	>10	**QND10**	>10	>10	>10
OCH_3	**PPRD11**	>10	>10	>10	**QND11**	6.7 ± 1.5[§]	>10	0.19 ± 0.09[§]
	PPRD12	>10	>10	2.6 ± 0.4[#]	**QND12**	0.92 ± 0.34	>10	0.021 ± 0.001

[a] K_d > 10 μM was indicated in the compounds that did not pass the initial screen. K_d of TTIn-1 is 4.3 μM for α7-nAChRs, >10 μM for α4β2-nAChRs, and 6.0 μM for $5HT_{3A}$ receptors. [#] $p < 0.05$ compared with IND1 for PPRD series; [§] $p < 0.05$ compared with IND8 for QND series.

Binding Affinity (1/K_d) or Dissociation Constant (K_d). Modifications at R_2 showed that the *anti*-triazoles in the QND series have higher affinity than the corresponding compounds in PPRD series for both α7-nAChRs and $5HT_{3A}$ receptors. K_d values of all compounds that passed the initial screening with LGIC receptors are shown in Table 3.

5.1.1. Mono- and Disubstituted Benzenes. Binding affinities to α7-nAChRs for compounds where one substituent on benzene is a H-bond donor (PPRD2 and PPRD8) appeared to be greater than those bearing H-bond acceptor (PPRD3) or heteroatom (PPRD13). The $-NH_2$ of PPRD2 and $-OH$ of PPRD8 resemble bioisosteres of the $-NH$ of indole; the K_d values of PPRD2 and PPRD8 are not significantly different from that of IND1. Since PPRD7 does not bind to all tested LGIC receptors, the larger biphenyl moiety cannot be accommodated in the interface binding pocket. An increase in K_d from steric hindrance is also observed in compounds bearing benzene ring with disubstitution, PPRD14 (K_d > 10

DOI: 10.1021/acschemneuro.5b00058
ACS Chem. Neurosci. 2015, 6, 1317−1330

Table 4. EC_{50} and K_A Values of PPRD Series[a]

	agonist EC_{50} ± SD (μM)		antagonist K_A ± SD (μM)		
compd	$\alpha7$	$5HT_{3A}$	$\alpha7$	$\alpha4\beta2$	$5HT_{3A}$
IND1	0.17 ± 0.05	>10		>10	>10
mono- and disubstituted benzenes					
PPRD2	0.38 ± 0.08	>10	–	>10	>10
PPRD3	15.0 ± 0.6$^{*,\#}$	>10	–	>10	>10
PPRD4	3.1 ± 0.8	>10	–	>10	>10
PPRD7	>10	>10	–	>10	>10
PPRD8	2.9 ± 0.7	–	–	>10	39.0 ± 2.7^{C}
PPRD13	17.8 ± 4.6$^{*,\#}$	>10	–	>10	>10
PPRD14	>10	–	>10	>10	1.4 ± 0.1^{C}
PPRD15	3.1 ± 0.2	–	–	>10	6.0 ± 1.5^{C}
bicyclic ring systems					
PPRD1	7.4 ± 0.7$^{\#}$	>10	–	>10	>10
PPRD5	1.1 ± 0.2	>10	–	>10	>10
PPRD6	>10	>10	–	>10	>10
PPRD9	12.9 ± 4.6$^{*,\#}$	–	–	10.5 ± 3.1^{C}, 25.5 ± 12.8^{NC}	15.1 ± 4.0^{C}, 56.2 ± 31.0^{NC}
PPRD10	>10	>10	11.6 ± 3.5^{C}, 18.9 ± 4.8^{NC}	>10	>10
PPRD11	–	>10	6.6 ± 2.2^{C}, 6.6 ± 1.7^{NC}	6.5 ± 1.7^{C}	>10
PPRD12	–	–	4.5 ± 1.5^{C}, 11.3 ± 4.5^{NC}	>10	2.2 ± 0.3^{C}

[a]Data were averaged from at least three independent experiments. All values are reported as means ± SD. EC_{50} and K_A > 10 μM were indicated for the compounds that did not pass the initial screen. *Partial agonist; ^{C}competitive antagonist; ^{NC}noncompetitive antagonist; $^{\#}p < 0.05$ compared with IND1. Values are calculated as described in Methods.

Table 5. EC_{50} and K_A Values of QND Series[a]

	agonist EC_{50} ± SD (μM)		antagonist K_A ± SD (μM)		
compd	$\alpha7$	$5HT_{3A}$	$\alpha7$	$\alpha4\beta2$	$5HT_{3A}$
IND8	0.028 ± 0.010	0.21 ± 0.08*	–	>10	–
mono- and disubstituted benzenes					
QND2	0.052 ± 0.018	1.6 ± 0.3*	–	>10	–
QND3	0.097 ± 0.025	5.7 ± 1.7*,§	–	>10	–
QND4	0.20 ± 0.08	–	–	>10	0.50 ± 0.27^{C}, 0.53 ± 0.18^{NC}
QND7	–	>10	6.7 ± 2.4^{C}, 26.2 ± 9.8^{NC}	>10	>10
QND8	0.037 ± 0.009	0.90 ± 0.09*	–	6.2 ± 1.7^{C}	–
QND13	1.0 ± 0.3§	4.9 ± 1.2§	–	11.2 ± 2.6^{C}, 22.7 ± 6.4^{NC}	–
QND15	1.3 ± 0.0§	0.26 ± 0.03*	–	11.6 ± 1.0^{C}	–
bicyclic ring systems					
QND1	0.12 ± 0.04	0.30 ± 0.04*	–	>10	–
QND5	0.26 ± 0.00	0.16 ± 0.04*	–	>10	–
QND6	22.1 ± 6.2*,§	>10	–	7.0 ± 4.5^{C}, 6.2 ± 0.4^{NC}	>10
QND9	1.0 ± 0.0	1.4 ± 0.5	–	5.2 ± 1.2^{C}, 6.5 ± 0.2^{NC}	–
QND10	29.5 ± 7.5*,§	>10	–	>10	>10
QND11	1.6 ± 0.4	–	–	9.3 ± 4.3^{C}, 36.8 ± 21.8^{NC}	0.081 ± 0.009^{NC}
QND12	0.45 ± 0.14	0.34 ± 0.13*	–	>10	–

[a]Data were averaged from at least three independent experiments. All values are reported as means ± SD. EC_{50} and K_A > 10 μM were indicated for the compounds that did not pass the initial screening. *partial agonist; ^{C}competitive antagonist; ^{NC}noncompetitive antagonist; $^{\S}p < 0.05$ compared with IND8. Values are calculated as described in Methods.

μM), but not for PPRD15 (K_d = 4.4 μM) when compared to corresponding compounds with monosubstitutions (PPRD8 and PPRD2). The modified compounds in the PPRD series were generally selective for $\alpha7$-nAChRs.

In the QND series, K_d's for $\alpha7$-nAChRs of six compounds where indole was replaced by mono- and disubstituted benzene are not significantly different from IND8, except for QND15. The K_d value of QND8 where the phenyl hydroxyl group acts as H-bond donor, similar to the −NH of indole, was found to be the lowest (0.081 μM). Most compounds in QND series that bind to $\alpha7$-nAChRs show binding to $5HT_{3A}$ receptors with K_d's in the range of 0.04−2.3 μM. The ester extension of QND15 increases the binding affinity to $5HT_{3A}$ receptor (K_d = 0.043 μM) that is lower than that for QND2, its corresponding structure (K_d = 1.2 μM) and equivalent to IND8 (K_d = 0.052 μM).

5.1.2. Bicyclic Ring Systems. The K_d values of all tested LGIC receptors of compounds in PPRD series that contain aromatic bicyclic systems increased when compared with IND1. Methylation of indole ring in PPRD9 and addition of carbonyl group in the indole ring in PPRD5 were found to increase $\alpha7$-nAChR K_d values (K_d = 12.1 and 3.3 μM, respectively). Changing the −NH indole orientation in the structures of

DOI: 10.1021/acschemneuro.5b00058
ACS Chem. Neurosci. 2015, 6, 1317−1330

PPRD11 and PPRD12 resulted in a reduction of binding affinity to α7-nAChRs.

For the QND series, the K_d's for α7-nAChRs of all compounds are higher than that for IND8 except for QND1 (K_d = 0.16 μM) and QND12 (K_d = 0.92 μM). Methylation of the indole ring led to a 15-fold increase in K_d of QND9 (K_d = 1.9 μM) when compared to IND8. Steric hindrance caused by acyl substitution on the indole ring (QND5, QND11) or methoxy substitution on the naphthalene ring (QND6) increased the α7-nAChR K_d from 0.1 μM to >2 μM. However, changing the orientation of the indole in QND12 did not affect the α7-nAChR K_d. For $\alpha4\beta2$-nAChRs, only two compounds, QND6 and QND9, showed similar K_d's to IND8. The K_d's of all modified compounds in the QND series for $5HT_{3A}$ receptors are same as IND8 except for QND11.

5.2. Effect of the Aromatic Moiety on Agonist and Antagonist Activity. The compounds in the QND series have higher α7 agonist potencies than PPRD series. The EC_{50} and K_A values of PPRD and QND series are shown in Tables 4 and 5, respectively.

5.2.1. Mono- and Disubstituted Benzenes. The potencies of compounds in PPRD series are in accord with their binding affinities (Table 4); the α7-nAChR dose–response curves are shown in Figure 5A. Compounds containing H-bond donor as a substituent (PPRD2 and PPRD8) have higher potency (0.38 and 2.9 μM) than those with H-bond acceptor (PPRD3) or heteroatom (PPRD13) (15 and 17.8 μM). Additional *m*-substitution decreased the potencies of PPRD14 (EC_{50} > 10 μM) and PPRD15 (EC_{50} = 3.1 μM) compared to the corresponding monosubstituted compounds, PPRD8 (EC_{50} = 2.9 μM) and PPRD2 (EC_{50} = 0.38 μM), respectively. Three compounds from this modified series also show competitive antagonism behavior to $5HT_{3A}$ receptors, that is, PPRD8, PPRD14, and PPRD15 (K_A = 39.0, 1.4, and 6.0 μM, respectively) (Supporting Information Figure S5).

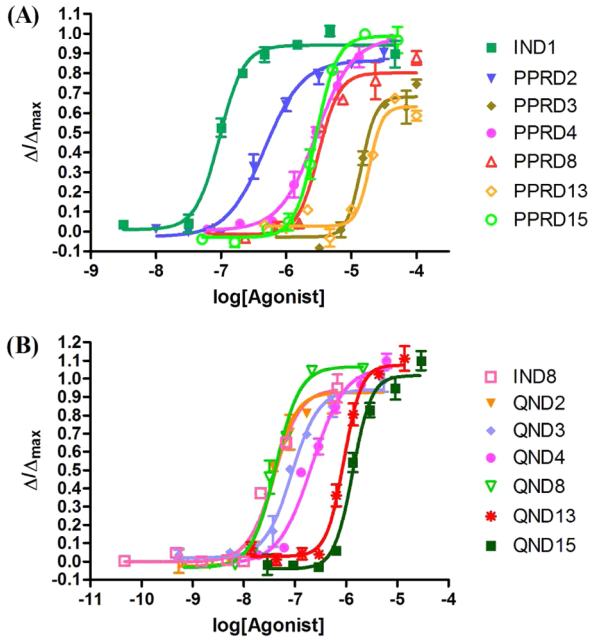

Figure 5. α7-nAChR agonist dose–response curves of mono- and disubstituted benzenes for (A) PPRD and (B) QND series. Assays were performed in the presence of 10 μM PNU-120596. FRET ratios were normalized to the maximum response with 100 nM (±)-epibatidine.

As shown in Figure 5B, the potencies of QND2 (EC_{50} = 0.052 μM), QND3 (EC_{50} = 0.097 μM), QND4 (EC_{50} = 0.20 μM), and QND8 (EC_{50} = 0.037 μM) are not significantly different from that of IND8 (EC_{50} = 0.028 μM). The heteroatom in QND13 and steric hindrance from additional methyl ester substituent in QND15 decreased α7-nAChR agonist potency (EC_{50} = 1.0 and 1.3 μM, respectively), while the more bulky biphenyl group turned QND7 into a weak α7-nAChR antagonist (Supporting Information Figure S6). Three compounds (QND8, QND13, QND15) showed moderate to low antagonist potencies for $\alpha4\beta2$-nAChRs (Supporting Information Figure S7). Interestingly, all compounds having heteroatom substitutions at *p*-position (QND2, QND3, QND8, QND13, QND15) have $5HT_{3A}$ receptor agonist properties in contrast to the $5HT_{3A}$ antagonist properties of TTIn-1 and QND4 (Supporting Information Figures S7 and S8).

5.2.2. Bicyclic Ring Systems. The functional responses of PPRD series that contain bicyclic amines are in agreement with data from the binding affinity analysis. Removal of H-bond donor, the –NH indole, markedly reduced the agonist EC_{50} of PPRD1 and PPRD9 compared to IND1 (Figure 6A). PPRD9 also acts $\alpha4\beta2$-nAChR and $5HT_{3A}$ receptor antagonists (Supporting Information Figure S10 and S5, respectively). Change in position of the NH-indole, the H-bond donor, turned PPRD11 and PPRD12 into weak and nonselective α7-nAChR antagonists (Supporting Information Figure S6).

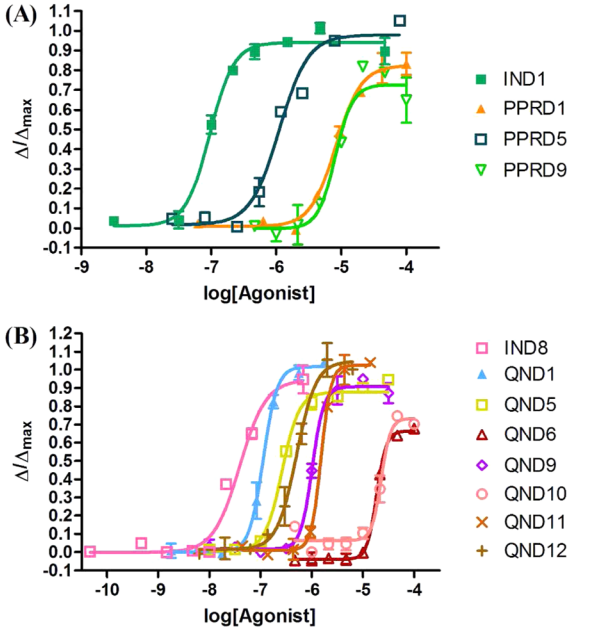

Figure 6. α7-nAChR agonist dose–response curves for indole modification, other bicyclic rings, and nitrogen-rich ring for (A) PPRD and (B) QND series. Assays were performed in the presence of 10 μM PNU-120596. FRET ratios were normalized to the maximum response by 100 nM (±)-epibatidine.

The α7 agonist properties of compounds in QND series showed a common pattern with the PPRD series. The potency and selectivity profiles for α7-nAChRs were not enhanced when compared with IND8. Compounds having heteroatom at *p*-position (QND1, QND5, QND9) and QND12 were $5HT_{3A}$

DOI: 10.1021/acschemneuro.5b00058
ACS Chem. Neurosci. 2015, 6, 1317–1330

agonists (Supporting Information Figure S8), whereas QND11 is a $5HT_{3A}$ antagonist (Supporting InformationFigure S9).

Replacement of the indole with an electron-rich adenine ring altered PPRD10 into α7-nAChR antagonist with moderate potency (K_A = 11.6[C], 18.9[NC] μM) (Supporting Information Figure S6), whereas QND10 showed modest α7-agonist activity (EC_{50} = 29.5 μM).

6. General Structure−Activity Considerations. All QND compounds have higher affinity and potency than the corresponding compounds in PPRD series. The activity profiles might arise from the rigidity of the quinuclidine ring that restricts the distance between the cationic center and the hydrogen bond acceptor in the triazole to the optimal 4.1 Å distance to N2 or 5.3 Å distance to N3, conferring key interactions in the binding pocket to achieve agonist properties. Also the quinuclidine compounds present a greater angle of access to form a hydrogen bond with the backbone carbonyl oxygen of Trp149 (α7 numbering). The hydrophobic R_2 is also an important motif affecting to the selectivity and potency profiles. The proper hydrophobic motifs for potent α7-nAChR agonists for 1,2,3-triazole based molecules appeared to be 5-substituted indole, benzodioxole, and their isosteric *p*-substituted benzene of small group, that is $-NH_2$, $-OCH_3$, $-CH_3$, and $-OH$. Information obtained from optimizing triazole derivatives via 43 compounds in three series (IND, PPRD, and QND series) revealed that the basic center with 3.7−3.8 Å length of linker, the triazole ring as H-bond acceptor, and the designated motif are the key pharmacophoric features of the triazole derivatives to become α7-nAChR agonists (Figure 7). This investigation also provides an analysis of

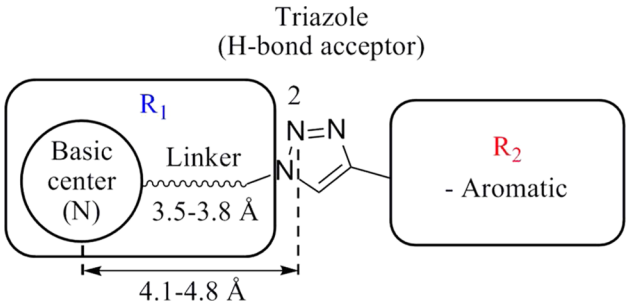

Figure 7. Pharmacophore model of α7-nAChR agonist obtained from this study.

specificity for α7-nAChR agonist activity in relation to the prevalent $\alpha4\beta2$-nAChR and the LGIC homologous $5HT_{3A}$ receptor. With the triazole series there is minimal overlap in potency with $\alpha4\beta2$-nAChR, and when observed, it is usually an α7 agonist versus an $\alpha4\beta2$ antagonist. A great parallelism is seen with α7 agonists and $5HT_3$ antagonists/agonists. However, it remains to be determined what complement of these two activities would be therapeutically advantageous.[36] Through high resolution crystallographic studies, it should be possible to investigate the binding poses, side chain positions and conformational differences torsional angles in the ligand bound complexes with AChBP in greater depth.[37]

The α7-nAChR agonist properties of the compounds in the three series of 1,4-disubstituted (*anti*) 1,2,3-triazoles verify that the triazole ring plays a role not only as the H-bond acceptor but as a linker for optimizing distance and orientation for key interactions: H-bond from basic amine with carbonyl backbone of conserved Trp, the H-bond with the triazole, and hydrophobic interactions in the binding pocket of α7-nAChR for α7-agonist action.

IND1, which has piperidine as the basic amine with a 2-methylene linker to triazole, is a selective and potent α7-nAChR agonist in the series. Its agonist potency is 3.5-fold higher than that of the lead compound TTIn-1 and is highly selective for α7 over $\alpha4\beta2$-nAChRs and the $5HT_{3A}$ receptors. IND8 with quinuclidine as the basic center is the most potent α7 agonist with a moderate selectivity profile: its α7 agonistic potency increases 20-fold from that of TTIn-1. Modification of the aromatic motifs in PPRD series did not further enhance affinity and potency profiles, whereas six compounds of QND series showed higher α7-nAChR agonistic potency than TTIn-1. However, alterations of the indole substitution reduced the selectivity profile with antagonism on $\alpha4\beta2$-nAChRs and antagonism/agonism on $5HT_{3A}$ receptors.

METHODS

1. General Experimental Detail. Chemical reagents are from Sigma-Aldrich, Oakwood, Alfa Aesar, Fluka, and Acros, whereas all solvents are from Fisher. All starting materials with at least 95% purity were used without further purification. The reactions were monitored by TLC and LC-MS (HP 1100 Series LC/MSD). Melting points of the final compounds were measured (Thomas-Hoover Unimelt), and the structures were elucidated by using FTIR (Thermo Scientific Nicolet iS5), NMR (Variance Mercury-300, Bruker AMX-400, Bruker DRX-500), and HRMS (Agilent ESI-TOF). Purity of final compounds was determined by chromatographic integration of the diode array UV acquired on an HP 1100 series LC/MSD combining liquid chromatography with electron spray ionization (ESI) mass spectrometry. Analyses were conducted using 30−100% MeCN/water containing 0.1% trifluoroacetic acid (TFA); all compounds were determined to be >95% purity. The physicochemical properties were predicted by MarvinSketch.

1.1. Azide Preparation (Scheme 1). When starting with amines, the azide building blocks were prepared by diazo transfer reaction[29] (IND1−IND3, IND5−IND10, IND14, PPRD1−PPRD15, QND1−QND13, QND15) whereas nucleophilic substitution was used for the molecules bearing good leaving groups,[30,31] that is, alicyclic alcohols (IND4 and IND11) and alkyl chlorides (IND12, IND13) (Scheme 1). All azido compounds were confirmed by LC-MS and used in CuAAC without further purification (more than 90% purity).

For diazo transfer reaction, the trifluoromethanesulfonyl azide (TfN_3) was prepared first by the reaction between trifluoromethanesulfonic anhydride and 5 equiv of sodium azide in the mixture of water and toluene. The reaction mixture was stirred vigorously at room temperature for 2 h and then extracted with toluene to obtain TfN_3. Then the primary amine was reacted with 1.8 equiv of freshly prepared TfN_3 in the mixture of H_2O/CH_3OH/toluene in the ratio of 3:6:5 at room temperature overnight to give the azido compound. The methylene linker of some azide building blocks (IND3, IND5, IND14) was extended before azidation. Starting amine 1.3 equiv was reacted with *N*-(2-bromoethyl) phthalimide, *N*-(3-bromopropyl)phthalimide, or *N*-(4-bromobutyl)phthalimide to vary the length of linker[38] using 2 equiv of triethylamine (Et_3N) as catalyst. The reaction was refluxed overnight in EtOH. Then, the phthalimide group was deprotected by refluxing with hydrazine monohydrate for 45 min to give the primary amine.

For nucleophilic substitution of alicyclic alcohols, the starting alcohol was mesylated first by 1.5 equiv of methanesulfonyl chloride (MsCl) using 1.6 equiv of Et_3N as a basic catalyst. The reaction mixture was run in CH_2Cl_2 from 0 °C to room temperature for 4 h to get mesylated alcohol. After that, this mesylated alcohol was refluxed with 1.2 equiv of sodium azide in MeCN for 6 h to obtain the azido compound.

For alkyl chlorides, the starting material was refluxed overnight with 3 equiv of sodium azide in water. After that, diethyl ether was added in the reaction mixture followed by 4 equiv of NaOH. The reaction

DOI: 10.1021/acschemneuro.5b00058
ACS Chem. Neurosci. 2015, 6, 1317−1330

mixture was stirred in an ice bath for 30 min. Then, the reaction mixture was extracted with diethyl ether, dried over $MgSO_4$ anhydrous, and concentrated in vacuo to obtain the azido compound.

1.2. Alkyne Preparation. The halogen containing molecule was reacted with 3 equiv of ethynyltrimethylsilane having $PdCl_2(PPh_3)_2$ (0.03−0.05 equiv), CuI (0.03−0.05 equiv) as catalyst, and Et_3N as base in DMF at room temperature under N_2 atmosphere for 3 h to overnight via the Sonogashira reaction. After extraction with diethyl ether or EtOAc and purification by column chromatography, the silyl group was removed by adding 1 M of TBAF in THF or K_2CO_3 in CH_3OH. The crude product was purified by column chromatography to give terminal alkyne products; for example, 5-ethynyl-1*H*-indole was prepared via method described above using 5-iodoindole as starting reagent and purified by column chromatography (10% EtOAc in hexane) to yield intermediate compound (90.39%). ^{1}H NMR (300 MHz, $CDCl_3$) δ 8.19 (s, 1H), 7.82 (s, 1H), 7.35−7.27 (m, 2H), 7.22−7.17 (m, 1H), 6.55−6.50 (m, 1H), 0.28 (s, 9H). ^{13}C NMR (76 MHz, $CDCl_3$) δ 135.6, 127.7, 126.1, 125.3, 125.2, 114.3, 111.1, 107.1, 103.0, 91.3, 0.3. After desilylation and purification (10% EtOAc in hexane), 5-ethynyl-1*H*-indole as yellow solid was obtained (79.19%). ^{1}H NMR (500 MHz, $CDCl_3$) δ 8.20 (s, 1H), 7.85 (s, 1H), 7.38−7.29 (m, 2H), 7.24−7.19 (m, 1H), 6.57−6.52 (m, 1H), 3.02 (s, 1H). ^{13}C NMR (126 MHz, $CDCl_3$) δ 135.8, 127.8, 126.1, 125.5, 125.3, 113.3, 111.2, 103.0, 85.4, 74.8.

1.3. Copper-Catalyzed Azide−Alkyne Cycloaddition (CuAAC). The azide building blocks were reacted with an alkyne building block (1:1) in a mixture of *t*-BuOH and water (1:1) using 5 mol % of $CuSO_4{\cdot}5H_2O$ and 20 mol % of sodium ascorbate as catalyst. The reaction mixture was run at room temperature for 2.5−24 h and purified by column chromatography; for example, 1-(2-azidoethyl)-piperidine (0.0641 g, 0.42 mmol) was reacted with 5-ethynyl-1*H*-indole (0.0499 g, 0.35 mmol) in a 1:1 ratio of *t*-BuOH and water with $CuSO_4{\cdot}5H_2O$ (0.0050 g, 0.02 mmol) and sodium ascorbate (0.0158 g, 0.08 mmol) as catalyst. The reaction was stirred at room temperature for 5 h. After that, the reaction mixture was extracted with CH_2Cl_2. The crude product was purified by column chromatography (EtOAc) to give a pale yellow solid compound of 5-(1-(2-(piperidin-1-yl)ethyl)-1*H*-1,2,3-triazol-4-yl)-1*H*-indole (IND1) (68.86%). FTIR (ATR) (cm^{-1}) 3318, 3148, 3083, 2924, 1615, 1547, 1452, 1438, 1346, 1225, 1121, 1054, 892, 795, 771, 745. ^{1}H NMR (500 MHz, DMSO-d_6) δ 8.41 (s, 1H), 8.00 (dd, J = 1.6, 0.8 Hz, 1H), 7.58 (dd, J = 8.4, 1.5 Hz, 1H), 7.44 (d, J = 8.4 Hz, 1H), 7.36 (dd, J = 2.9, 2.2 Hz, 1H), 6.50−6.44 (m, 1H), 4.48 (t, J = 6.5 Hz, 2H), 2.76 (t, J = 6.5 Hz, 2H), 2.47−2.34 (m, 4H), 1.51−1.44 (m, 4H), 1.42−1.33 (m, 2H). ^{13}C NMR (126 MHz, DMSO-d_6) δ 147.7, 135.6, 127.8, 126.0, 122.0, 120.3, 119.0, 116.7, 111.7, 101.4, 57.8, 53.8, 47.0, 25.5, 23.9; mp = 148−149 °C. HRMS calculated ($C_{17}H_{21}N_5$, MH^+) 296.1871, found 296.1871.

2. Activity Testing. Cell lines expressing specific subtypes of receptors and a genetically encoded fluorescence resonance energy transfer (FRET)-based calcium sensor (TN-XXL) were prepared from sequential transfections and clone selection.[33] Human α7-nAChRs and $\alpha4\beta2$-nAChRs were expressed in HEKtsA201 cells, whereas hα7/m5HT_{3A} chimeric receptors and mouse 5HT_{3A} receptors were expressed in HEK293 cells. Cells were cultured in DMEM (Corning, Cellgro, Manassas, VA) supplemented with 10% FBS (Gibco, Life Technologies, Grand Island, NY) and 1% glutamine (Gibco, Life Technologies, Grand Island, NY) and incubated at 37 °C with 10% CO_2.

2.1. Intact Cell Binding Assay. Cell based neurotransmitter fluorescent engineered reporters (CNiFERs) expressing Ca^{2+} permeable LGIC receptors were used to determine the K_d values of the compounds. Cells were harvested by centrifugation (Beckman coulter, Brea, CA) at 500 rpm for 5 min, and then mixed and incubated on ice for 30 min, after counting, with Wheat Germ Agglutinin SPA beads (20 mg/mL) (PerkinElmer, Waltham, MA) in Hank's balanced salt solution (HBSS) (Gibco, Life Technologies, Grand Island, NY) at the specified concentrations: (1) hα7/m5HT_{3A} chimera-TN-XXL, 200 000 cells/well, 1 mg/mL SPA beads; (2) h$\alpha4\beta2$-TN-XXL, 100 000 cells/well, 0.5 mg/mL SPA beads; and (3) m5HT_{3A}-TN-XXL, 100 000 cells/well, 1 mg/mL SPA beads. The compounds were initially screened at 10 μM final concentration. Nonspecific binding was measured by using 100 μM MLA (Tocris Bioscience, Bristol, U.K.) for α7/5HT_{3A} chimeric receptors, 10 μM varenicline (Tocris Bioscience, Bristol, U.K.) for $\alpha4\beta2$-nAChR, and 300 nM tropisetron (Tocris Bioscience, Bristol, U.K.) for 5HT_{3A} receptors. After that, the radioactive ligands were added at 20 nM final concentration of [^{3}H]-(±)-epibatidine for α7/5HT_{3A} chimeric receptors, 5 nM [^{3}H]-(±)-epibatidine for $\alpha4\beta2$-nAChR, and 10 nM [^{3}H]-granisetron for 5HT_{3A} receptors. The mixtures were measured on the Wallac 1450 MicroBeta Trilux with 1 h intervals for a total of 15 measurements. Compounds that displaced over 50% of the bound radioligand from the LGIC-CNiFERs were analyzed in separate experiments for K_d values by the Cheng-Prusoff equation using GraphPad Prism. Mean K_d values and standard deviations were calculated from at least three independent experiments. The difference of K_d values were statistically analyzed by one-way ANOVA followed by Tukey's multiple comparison test using GraphPad Prism.

2.2. Functional Assays for Agonists and Antagonists.[33] Agonist and antagonist elicited responses were characterized using the above CNiFER cell expressing LGIC receptors. A fluorometric imaging plate reader system (FlexStation 3; Molecular Devices, Sunnyvale, CA) was used to detect FRET responses from HEK cells expressed α7-nAChRs, $\alpha4\beta2$-nAChRs, and 5HT_{3A} receptors. A 96-well black, clear-bottom microplate (Greiner bio-one, Germany) was coated with poly-D-lysine (Sigma-Aldrich, St. Louis, MO) at 50 μL/well for 30 min and then washed with phosphate-buffered saline (PBS) (Corning, Cellgro, Manassas, VA) before plating the cells. After plating and incubation at 37 °C for 1 day, the media was replaced with 100 μL of artificial cerebrospinal fluid (aCSF: 121 mM NaCl, 5 mM KCl, 26 mM $NaHCO_3$, 1.2 mM $NaH_2PO_4{\cdot}H_2O$, 10 mM glucose, 2.4 mM $CaCl_2$, 1.3 mM $MgSO_4$, 5 mM HEPES, pH 7.4) for $\alpha4\beta2$ and 5HT_{3A} receptors, whereas 10 μM PNU-120596 (Tocris Bioscience, Bristol, U.K.) in aCSF with 30 min incubation at 37 °C was used for α7-nAChR. The tested compounds were prepared in aCSF for all receptors except α7-nAChR, where 10 μM PNU-120596, a positive allosteric modulator (PAM), was used. The prepared compounds were added in a separate 96-well polypropylene plate (Costar, Corning, NY). Experiments were conducted at 37 °C using 436 nm excitation. Emitted light was collected at 485 and 528 nm. Basal fluorescence was recorded for 30 s, followed by addition of 50 μL of ligand (first addition). Measurements were made at 3.84 s intervals for 2 min to measure the agonist response. After that, the agonist compound, which was 100 nM final concentration of (±)-epibatidine (Tocris Bioscience, Bristol, U.K.) for α7- and $\alpha4\beta2$-nAChRs, and 1 μM of 5-hydroxytryptamine (5-HT) (Tocris Bioscience, Bristol, U.K.) for the 5HT_{3A} receptor were added to evaluate the antagonist response of the test compounds. Agonist and antagonist properties were sequentially screened at the final concentration of 13.3 and 10 μM, respectively, which differed from the screening concentration from intact cell binding assay (10 μM). Therefore, some compounds that do not bind to LGIC receptors at screening concentrations still exhibit agonist and antagonist responses in functional screening characterizations. Compounds whose fraction of the maximal response (Δ/Δ_{max}) was higher than 0.20 were further evaluated to determine their EC_{50}, whereas compounds that inhibit Δ/Δ_{max} more than 0.50 were further characterized to determine the type of antagonism and also calculate the antagonist dissociation constant (K_A). The K_A for competitive antagonists and noncompetitive antagonists were calculated from the Schild eqs 1 and 2.

$$K_A = [A]/[DR - 1] \quad (1)$$

$$K_A = [A]/[(\Delta_{max}/\Delta) - 1] \quad (2)$$

where [A] is the concentration of compound, DR (dose ratio) is the EC_{50} ratio of tested compound over the control compound, which is (±)-epibatidine for α7- and $\alpha4\beta2$-nAChR, and 5HT for 5HT_{3A}, and Δ/Δ_{max} is the fraction of the maximal response. Mean values and standard deviations were calculated from at least three independent experiments. The difference of EC_{50} and K_A values were statistically

DOI: 10.1021/acschemneuro.5b00058
ACS Chem. Neurosci. 2015, 6, 1317−1330

analyzed by one-way ANOVA followed by Tukey's multiple comparison test using GraphPad Prism.

■ ASSOCIATED CONTENT

Supporting Information

Synthesis and characterization of alkyne and 1,2,3-triazoles. Sequence alignment of human α7-nAChR with human and mouse $5HT_{3A}$ receptors (Figure S1). IND, PPRD, and QND series dose−response curve of $\alpha4\beta2$-nAChRs and $5HT_{3A}$ receptors (Figures S2−S10). The Supporting Information is available free of charge on the ACS Publications website at DOI: 10.1021/acschemneuro.5b00058.

■ AUTHOR INFORMATION

Corresponding Author

*Phone: 662 6448695. E-mail: opa.vaj@mahidol.ac.th.

Author Contributions

Study conception and design: K.A., V.V.F., O.V., and P.T.. Acquisition of data: K.A. Analysis and interpretation of data: K.A. Drafting of manuscript: K.A. Critical revision: K.A., V.V.F., O.V., and P.T.

Funding

This work was supported by Thailand Research Fund (TRF) through the Royal Golden Jubilee Ph.D. Program (Grant No. PHD/0113/2551) to K.A. and O.V., the Office of the High Education Commission and Mahidol University under the National Research Universities to O.V., National Institutes of Health GM18360 to P.T., and GM087620 to V.V.F.

Notes

The authors declare no competing financial interest.

■ ACKNOWLEDGMENTS

We acknowledge Dr. Ida Drier, Dr. Rakesh Sit, and Dr. James Oakdale for providing some synthesis materials and advice, and Dr. Akos Nemecz for suggestions on the pharmacological evaluation.

■ ABBREVIATIONS

5HT, 5-hydroxytryptamine; AChBP, acetylcholine binding protein; aCSF, artificial cerebrospinal fluid; AD, Alzheimer's disease; BBB, blood-brain barrier; CNiFERs, cell based neurotransmitter fluorescent engineered reporters; CuAAC, copper-catalyzed azide−alkyne cycloaddition; DMEM, Dulbecco's modified Eagle's medium; DR, dose−response; ESI, electrospray ionization; FRET, fluorescence resonance energy transfer; FTIR, Fourier transform infrared spectroscopy; HBSS, Hank's balanced salt solution; HRMS, high resolution mass spectrometry; LC-MS, liquid chromatography mass spectrometry; LGIC, ligand-gated ion channel; *Ls*, *Lymnaea stagnalis*; MLA, methyllycaconitine; nAChR, nicotinic acetylcholine receptor; NMR, nuclear magnetic resonance; RBA, radioligand binding assay; SPA, signal proximity assay

■ REFERENCES

(1) Gotti, C., and Clementi, F. (2004) Neuronal nicotinic receptors: from structure to pathology. *Prog. Neurobiol. 74* (6), 363−396.

(2) Dani, J. A., and Bertrand, D. (2007) Nicotinic acetylcholine receptors and nicotinic cholinergic mechanisms of the central nervous system. *Annu. Rev. Pharmacol. Toxicol. 47*, 699−729.

(3) Gotti, C., Zoli, M., and Clementi, F. (2006) Brain nicotinic acetylcholine receptors: native subtypes and their relevance. *Trends Pharmacol. Sci. 27* (9), 482−491.

(4) Schaaf, C. P. (2014) Nicotinic acetylcholine receptors in human genetic disease. *Genet. Med. 16* (9), 649−656.

(5) Jensen, A. A., Frolund, B., Liljefors, T., and Krogsgaard-Larsen, P. (2005) Neuronal nicotinic acetylcholine receptors: structural revelations, target identifications, and therapeutic inspirations. *J. Med. Chem. 48* (15), 4705−4745.

(6) Gaimarri, A., Moretti, M., Riganti, L., Zanardi, A., Clementi, F., and Gotti, C. (2007) Regulation of neuronal nicotinic receptor traffic and expression. *Brain Res. Rev. 55* (1), 134−143.

(7) Lippiello, P., Bencherif, M., Hauser, T., Jordan, K., Letchworth, S., and Mazurov, A. (2007) Nicotinic receptors as targets for therapeutic discovery. *Expert Opin. Drug Discovery 2* (9), 1185−1203.

(8) Taly, A., Corringer, P. J., Guedin, D., Lestage, P., and Changeux, J. P. (2009) Nicotinic receptors: allosteric transitions and therapeutic targets in the nervous system. *Nat. Rev. Drug Discovery 8* (9), 733−750.

(9) Briggs, C. A., Anderson, D. J., Brioni, J. D., Buccafusco, J. J., Buckley, M. J., Campbell, J. E., Decker, M. W., Donnelly-Roberts, D., Elliott, R. L., Gopalakrishnan, M., Holladay, M. W., Hui, Y. H., Jackson, W. J., Kim, D. J., Marsh, K. C., O'Neill, A., Prendergast, M. A., Ryther, K. B., Sullivan, J. P., and Arneric, S. P. (1997) Functional characterization of the novel neuronal nicotinic acetylcholine receptor ligand GTS-21 in vitro and in vivo. *Pharmacol., Biochem. Behav. 57* (1−2), 231−241.

(10) Hibbs, R. E., Sulzenbacher, G., Shi, J., Talley, T. T., Conrod, S., Kem, W. R., Taylor, P., Marchot, P., and Bourne, Y. (2009) Structural determinants for interaction of partial agonists with acetylcholine binding protein and neuronal alpha7 nicotinic acetylcholine receptor. *EMBO J. 28* (19), 3040−3051.

(11) Wallace, T. L., Callahan, P. M., Tehim, A., Bertrand, D., Tombaugh, G., Wang, S., Xie, W., Rowe, W. B., Ong, V., Graham, E., Terry, A. V., Jr., Rodefer, J. S., Herbert, B., Murray, M., Porter, R., Santarelli, L., and Lowe, D. A. (2011) RG3487, a novel nicotinic alpha7 receptor partial agonist, improves cognition and sensorimotor gating in rodents. *J. Pharmacol. Exp. Ther. 336* (1), 242−253.

(12) Toyohara, J., and Hashimoto, K. (2010) alpha7 Nicotinic Receptor Agonists: Potential Therapeutic Drugs for Treatment of Cognitive Impairments in Schizophrenia and Alzheimer's Disease. *Open Med. Chem. J. 4*, 37−56.

(13) Vicens, P., Ribes, D., Torrente, M., and Domingo, J. L. (2011) Behavioral effects of PNU-282987, an alpha7 nicotinic receptor agonist, in mice. *Behav Brain Res. 216* (1), 341−348.

(14) Mazurov, A., Hauser, T., and Miller, C. H. (2006) Selective alpha7 nicotinic acetylcholine receptor ligands. *Curr. Med. Chem. 13* (13), 1567−1584.

(15) Radek, R. J., Robb, H. M., Stevens, K. E., Gopalakrishnan, M., and Bitner, R. S. (2012) Effects of the novel alpha7 nicotinic acetylcholine receptor agonist ABT-107 on sensory gating in DBA/2 mice: pharmacodynamic characterization. *J. Pharmacol. Exp. Ther. 343* (3), 736−745.

(16) Ghiron, C., Haydar, S. N., Aschmies, S., Bothmann, H., Castaldo, C., Cocconcelli, G., Comery, T. A., Di, L., Dunlop, J., Lock, T., Kramer, A., Kowal, D., Jow, F., Grauer, S., Harrison, B., La Rosa, S., Maccari, L., Marquis, K. L., Micco, I., Nencini, A., Quinn, J., Robichaud, A. J., Roncarati, R., Scali, C., Terstappen, G. C., Turlizzi, E., Valacchi, M., Varrone, M., Zanaletti, R., and Zanelli, U. (2010) Novel alpha-7 nicotinic acetylcholine receptor agonists containing a urea moiety: identification and characterization of the potent, selective, and orally efficacious agonist 1-[6-(4-fluorophenyl)pyridin-3-yl]-3-(4-piperidin-1-ylbutyl) urea (SEN34625/WYE-103914). *J. Med. Chem. 53* (11), 4379−4389.

(17) Horenstein, N. A., Leonik, F. M., and Papke, R. L. (2008) Multiple pharmacophores for the selective activation of nicotinic alpha7-type acetylcholine receptors. *Mol. Pharmacol. 74* (6), 1496−1511.

(18) Bunnelle, W. H., Dart, M. J., and Schrimpf, M. R. (2004) Design of ligands for the nicotinic acetylcholine receptors: the quest for selectivity. *Curr. Top Med. Chem. 4* (3), 299−334.

(19) Mazurov, A. A., Speake, J. D., and Yohannes, D. (2011) Discovery and development of alpha7 nicotinic acetylcholine receptor modulators. *J. Med. Chem. 54* (23), 7943−7961.
(20) Grimster, N. P., Stump, B., Fotsing, J. R., Weide, T., Talley, T. T., Yamauchi, J. G., Nemecz, A., Kim, C., Ho, K. Y., Sharpless, K. B., Taylor, P., and Fokin, V. V. (2012) Generation of candidate ligands for nicotinic acetylcholine receptors via in situ click chemistry with a soluble acetylcholine binding protein template. *J. Am. Chem. Soc. 134* (15), 6732−6740.
(21) Yamauchi, J. G., Gomez, K., Grimster, N., Dufouil, M., Nemecz, A., Fotsing, J. R., Ho, K. Y., Talley, T. T., Sharpless, K. B., Fokin, V. V., and Taylor, P. (2012) Synthesis of selective agonists for the alpha7 nicotinic acetylcholine receptor with in situ click-chemistry on acetylcholine-binding protein templates. *Mol. Pharmacol. 82* (4), 687−699.
(22) Hein, C. D., Liu, X. M., and Wang, D. (2008) Click chemistry, a powerful tool for pharmaceutical sciences. *Pharm. Res. 25* (10), 2216−2230.
(23) Rostovtsev, V. V., Green, L. G., Fokin, V. V., and Sharpless, K. B. (2002) A stepwise huisgen cycloaddition process: copper(I)-catalyzed regioselective "ligation" of azides and terminal alkynes. *Angew. Chem., Int. Ed. Engl. 41* (14), 2596−2599.
(24) Pin, F., Vercouillie, J., Ouach, A., Mavel, S., Gulhan, Z., Chicheri, G., Jarry, C., Massip, S., Deloye, J. B., Guilloteau, D., Suzenet, F., Chalon, S., and Routier, S. (2014) Design of alpha7 nicotinic acetylcholine receptor ligands in quinuclidine, tropane and quinazoline series. Chemistry, molecular modeling, radiochemistry, in vitro and in rats evaluations of a [(18)F] quinuclidine derivative. *Eur. J. Med. Chem. 82*, 214−224.
(25) Routier, S., Suzenet, F., Pin, F., Chalon, S., Vercouillie, J., and Guilloteau, D. (2014) 1,4-disubstituted 1,2,3-triazoles, methods for preparing same, and diagnostic and therapeutic uses thereof. U.S. Patent US 20140030191 A1.
(26) Rucktooa, P., Smit, A. B., and Sixma, T. K. (2009) Insight in nAChR subtype selectivity from AChBP crystal structures. *Biochem. Pharmacol. 78* (7), 777−787.
(27) Celie, P. H., van Rossum-Fikkert, S. E., van Dijk, W. J., Brejc, K., Smit, A. B., and Sixma, T. K. (2004) Nicotine and carbamylcholine binding to nicotinic acetylcholine receptors as studied in AChBP crystal structures. *Neuron 41* (6), 907−914.
(28) Hansen, S. B., Sulzenbacher, G., Huxford, T., Marchot, P., Taylor, P., and Bourne, Y. (2005) Structures of Aplysia AChBP complexes with nicotinic agonists and antagonists reveal distinctive binding interfaces and conformations. *EMBO J. 24* (20), 3635−3646.
(29) Beckmann, H. S., and Wittmann, V. (2007) One-pot procedure for diazo transfer and azide-alkyne cycloaddition: triazole linkages from amines. *Org. Lett. 9* (1), 1−4.
(30) Suzuki, T., Ota, Y., Ri, M., Bando, M., Gotoh, A., Itoh, Y., Tsumoto, H., Tatum, P. R., Mizukami, T., Nakagawa, H., Iida, S., Ueda, R., Shirahige, K., and Miyata, N. (2012) Rapid discovery of highly potent and selective inhibitors of histone deacetylase 8 using click chemistry to generate candidate libraries. *J. Med. Chem. 55* (22), 9562−9575.
(31) Dimitrov, I., Jankova, K., and Hvilsted, S. (2010) Synthesis of polystyrene-based random copolymers with balanced number of basic or acidic functional groups. *J. Polym. Sci., Part A: Polym. Chem. 48* (9), 2044−2052.
(32) Md Tohid, S. F., Ziedan, N. I., Stefanelli, F., Fogli, S., and Westwell, A. D. (2012) Synthesis and evaluation of indole-containing 3,5-diarylisoxazoles as potential pro-apoptotic antitumour agents. *Eur. J. Med. Chem. 56*, 263−270.
(33) Yamauchi, J. G., Nemecz, A., Nguyen, Q. T., Muller, A., Schroeder, L. F., Talley, T. T., Lindstrom, J., Kleinfeld, D., and Taylor, P. (2011) Characterizing ligand-gated ion channel receptors with genetically encoded Ca2++ sensors. *PLoS One 6* (1), e16519.
(34) Broad, L. M., Felthouse, C., Zwart, R., McPhie, G. I., Pearson, K. H., Craig, P. J., Wallace, L., Broadmore, R. J., Boot, J. R., Keenan, M., Baker, S. R., and Sher, E. (2002) PSAB-OFP, a selective alpha 7 nicotinic receptor agonist, is also a potent agonist of the 5-HT3 receptor. *Eur. J. Pharmacol. 452* (2), 137−144.
(35) Yamauchi, J. G. (2012) *Approaches in developing selective pharmacological lead compounds for the alpha7 nicotinic acetylcholine receptor with click-chemistry*. Ph.D. Dissertation, University of California, San Diego, CA.
(36) Hashimoto, K. (2015) Tropisetron and its targets in Alzheimer's disease. *Expert Opin. Ther Targets 19* (1), 1−5.
(37) Kaczanowska, K., Harel, M., Radic, Z., Changeux, J. P., Finn, M. G., and Taylor, P. (2014) Structural basis for cooperative interactions of substituted 2-aminopyrimidines with the acetylcholine binding protein. *Proc. Natl. Acad. Sci. U. S. A. 111* (29), 10749−10754.
(38) Coppo, F. T., Maskell, E. S. L., Redshaw, S., Skidmore, J., Ward, R. W., and Wilson, D. M. (2007) 2-Phenyl-5-amino-1,3,4-oxadiazoles and their use as nicotinic acetylcholine receptor ligands. European Patent WO2007138033.

DOI: 10.1021/acschemneuro.5b00058
ACS Chem. Neurosci. 2015, 6, 1317−1330